

# Bioelectrorheological model of the cell

## 3. Viscoelastic shear deformation of the membrane

Jarosław Poznański, Piotr Pawłowski, and Magdalena Fikus

Department of Biophysics, Institute of Biochemistry and Biophysics, Polish Academy of Sciences, 02-532 Warsaw, Poland

**ABSTRACT** An analytical electromechanical model of a spherical cell exposed to an alternating electric field was used to calculate shear stress generated in the cellular membrane. Shape deformation of *Neurospora crassa* (slime) spheroplasts was measured. Statistical analysis permitted empirical evaluation of creep of the cellular membrane within the range of infinitesimal stress. Final results were discussed in terms of various rheological models.

### INTRODUCTION

Early studies in cellular rheology have concentrated on investigations of human red blood cells (RBC) which owing to their specific morphology have been used as a simplified cellular model. They respond to mechanical stress in a rather uniform manner; their rheological parameters allow for a distinction between young and aged cells (Nash and Meiselman, 1983, Waugh, 1987). Moreover, the mechanical behavior of RBC taken from patients with certain diseases distinguishes them from RBC of healthy donors (Waugh and Agre, 1988). Contrary to RBC, most of the eukaryotic cells have a more complex internal structure manifested by the considerable dispersion in their rheological properties.

Modeling of cellular rheological phenomena calls for simplified assumptions. For example, Skalak et al. (1984) have treated the cell (leukocyte) as a homogeneous viscoelastic sphere. Viscoelastic properties manifested by a cell under specified experimental conditions can be attributed as well to the cellular membrane, which can be regarded as a thin spherical shell. This approach overlooks the real sources of viscoelasticity arising not only from the structural complexity of the membrane, but also from membrane interactions with cellular structures such as the cytoskeleton, internal membranes and organelles. This approach allows, however, for a description of a real object by the use of an effective model, and discloses the macroscopic behavior of the cell under stress.

There are many techniques for studying the mechanical properties of cells and cellular membranes (Evans and Skalak, 1980). More recently, a new procedure for studies of cell deformation in an external alternating electric field of high frequency has been developed (Sackmann et al., 1984, Barnaby et al., 1988, Engelhardt

and Sackmann, 1988, Fikus, 1988, Pawłowski and Fikus, 1989, Fikus and Pawłowski, 1989).

In the present study, the previously established analysis of shear stress in the viscoelastic shell surrounding a nonviscous, noncompressible internal medium (Pawłowski and Fikus, 1991) was applied in the case of a cell exposed to periodic electric field. The choice of the model, composed of three media with special emphasis on the shell is supported by the physical mechanism of stress generation by an alternating electric field on the shell surface.

The experiments presented below were aimed at determining the rheological parameters of the so-called standard population.

Rheological studies of cellular populations can be carried out in two ways:

(a) It is possible to fit a given rheological model to the temporal trajectory of deformation of each individual cell (Skalak et al., 1984) and then, by applying the  $\chi^2$  test to accept or discard the postulated model. For each cell a set of its rheological parameters is obtained. Because the fitting parameters of the constitutive equations are strongly correlated (correlation coefficients in the range of 0.8), subsequent averaging of rheological parameters for all cells results in drastic overestimation of their dispersion.

(b) The averaged creep function for all cells can be obtained. It is not a single curve but an area of distribution within which most of the single cells' creep function trajectories fall. At this stage of the procedure, it is possible to distinguish subpopulations of cells characterized by similar rheological behavior. Application of the  $\chi^2$  test helps in the subsequent choice of an appropriate rheological model for the population and, eventually, for subpopulations, if found. This procedure reduces statistical errors, making the evaluated final

Address correspondence to Dr. Fikus.

rheological parameters for a given cell population more reliable, and was followed in this study.

It was assumed that within the limits of controllable experimental conditions the analyzed population was homogeneous. Considerable scattering of the experimental data was observed, reflecting the influence of uncontrollable parameters on the process. In our opinion, this scattering was mainly due to the biological diversity of the cells such as the stage of their generation cycle, metabolic activity, individual structural complexity and so on. The general averaged characteristics of the cell population found by this approach should be treated as a starting point for further studies of various single-cell behaviors (sometimes extremely different from the general model), for comparative studies of cells in which the standard state has been disturbed, finally for studies of populations of different types of cells. Such investigations could in principle help to clarify the role of as yet uncontrollable parameters on the rheological properties of individual cells.

Nonlinear dependence of measured deformations on analytically determined stress was observed. It is well known that most physical processes can be correctly analytically described only when their relevant parameters show linear dependence. In this work, for the first time, a statistical procedure of data evaluation, including evaluation of variance, is proposed, which permits extrapolation of experimental data down to the limits of linear dependence of the infinitesimal deformation on the infinitesimal stress. This extrapolation procedure formally justifies the calculations of stress for an undeformed, spherical cell. A generalized description of the rheological behavior of a population under undamaging stress, utilizing linear equations, was obtained.

Spheroplasts of *Neurospora crassa* (slime) were used for exemplification of the procedure. These eukaryotic cells have previously been well characterized structurally and biochemically (Emerson, 1963, Scarborough, 1978, Aaronson and Martin, 1983), as well as with respect to their electrical properties (Fikus et al., 1987, Marszałek et al., 1989, 1991). They represent a convenient model for investigations of the native cytoplasmic membrane with no need for enzymatic pretreatment. This study introduces a new taxonomic group of organisms into the field of cellular rheology.

## THEORETICAL ANALYSIS OF STRESS AND DEFORMATION

### Model of a spherical shell

The analysis of the biorheological model of cell (Pawłowski and Fikus, 1989) was further extended (Pawłowski and Fikus, 1991). In this paper, shape

deformation of the thin area, noncompressible spherical shell, separating two different ideal liquids, exposed to an external, alternating electric field has been considered. It has been assumed that shear stress in the plane of the shell develops as a result of Maxwell stress acting on both shell surfaces. All media have been considered with losses (dielectric losses, conducting media). The foregoing analysis can be applied to a description of cell deformation.

For a cell meeting the requirements of the above model the  $z$  dimension parallel to field lines varies according to the formula:

$$(z - R)/R = 2\epsilon_s^{\text{extr}}, \quad (1)$$

where  $z$  is the cell demi-axis in the field direction,  $R$  is the initial cell radius and  $\epsilon_s^{\text{extr}}$  is the extreme shear deformation in the membrane plane.

Accordingly, the constitutive equation for shear elastic deformation relates  $\epsilon_s^{\text{extr}}$  and extreme shear stress in the membrane plane,  $\sigma_s^{\text{extr}}$ :

$$\epsilon_s^{\text{extr}} = \frac{1}{2\mu} \sigma_s^{\text{extr}}, \quad (2)$$

where  $\mu$  is the area elastic shear modulus which may be regarded as an effective elastic shear modulus (see next section), which describes the nondissipative phenomena. In a real situation, deformation of the cellular membrane under stress develops in time, owing to membrane viscosity. Hence, Eq. 2 is substituted by a constitutive equation for shear viscoelastic deformation:

$$\epsilon_s^{\text{extr}}(t) = \frac{1}{2} \int_0^t J(t - \tau) \frac{d\sigma_s^{\text{extr}}}{d\tau} d\tau, \quad (3)$$

where  $J(t - \tau)$  is a function of the viscoelastic shear response in the membrane plane after time  $(t - \tau)$  to a change in shear stress at time  $\tau$ .

The stress "jump" applied to the experiments can be expressed as a function of time:

$$\sigma_s^{\text{extr}}(\tau) = \sigma_s^{\text{extr}}(\text{init})\Theta(\tau) + \Delta\sigma_s^{\text{extr}}(\Theta(\tau - t_\uparrow) - \Theta(\tau - t^\downarrow)) \quad (4)$$

where  $\sigma_s^{\text{extr}}(\text{init})$  denotes the initial shear stress,  $t_\uparrow$  is the moment of the "jump" increase in shear stress,  $t^\downarrow$  is the moment of reversion to the initial shear stress,  $\Delta\sigma_s^{\text{extr}}$  is the increment of shear stress,  $\Theta(\tau)$  is the theta-Heaviside step function.

Upon use of Eqs. (3 and 4), evolution of shear deformation is obtained:

$$\epsilon_s^{\text{extr}} = \begin{cases} \frac{1}{2}J(t)\sigma_s^{\text{extr}}(\text{init}) & t < t_\uparrow \\ \frac{1}{2}J(t)\sigma_s^{\text{extr}}(\text{init}) + \frac{1}{2}J(t - t_\uparrow)\Delta\sigma_s^{\text{extr}} & t_\uparrow < t < t^\downarrow \\ \frac{1}{2}J(t)\sigma_s^{\text{extr}}(\text{init}) + \frac{1}{2}(J(t - t_\uparrow) - J(t - t^\downarrow))\Delta\sigma_s^{\text{extr}} & t > t^\downarrow \end{cases} \quad (5)$$

Experiments started when initial deformation,  $J(t)\sigma_s^{\text{extr}}(\text{init})$ , caused by the initial stress, became stabilized. Hence temporal evolution of initial deformation was not considered in the analysis:

$$J(t)\sigma_s^{\text{extr}}(\text{init}) = \frac{z(\text{init}) - R}{R} \text{ for } t_{\uparrow} - \delta < t, \quad (6)$$

where  $\sigma$  is the left-side environment of  $t_{\uparrow}$ , where deformation does not vary with time.

Upon use of Eqs. (1, 5, and 6), the description of cell length variation with time assumes the form:

$$\text{rel}(t) = \text{res}(t)\Delta\sigma_s^{\text{extr}}, \quad (7)$$

where:

$$\text{res}(t) = \begin{cases} 0 & t_{\uparrow} - \delta < t < t_{\uparrow} \\ J(t - t_{\uparrow}) & t_{\uparrow} < t < t^{\downarrow} \\ J(t - t_{\uparrow}) - J(t - t^{\downarrow}) & t^{\downarrow} < t, \end{cases} \quad (8)$$

and

$$\text{rel}(t) = \frac{z(t) - z(\text{init})}{R} \quad (9)$$

denotes the relative increase in cell length along electric field lines. It was directly measured for deformed cells.

### Effective model of cellular membrane

Assumptions of the above model were applied to the case of a spherical shell. This model can be used in description of more complex objects, when apparent effective properties of the surrounding shell (membrane) are considered. Thus, the shear elastic properties of the membrane depend on: (a) the elastic properties of the lipid bilayer with surface and integral proteins, together with a cushion of the membrane skeleton, (b) surface tension, and (c) interactions of the membrane with cytoplasm and internal skeleton. Effective shear elasticity can be expressed as a sum of elasticities:

$$\mu = \mu_s + c_1 \frac{\tau_0}{d} + c_2 \frac{R}{d} \mu_i, \quad (10)$$

where:  $\mu_s$  is shear elastic modulus of the membrane,  $\tau_0$  is surface tension,  $\mu_i$  is shear elastic modulus of the cell interior,  $d$  is membrane thickness,  $R$  is cell radius,  $c_1$  and  $c_2$  are numerical coefficients.

Upon solution of equilibrium equations for an elastic membrane exposed to external electric field,  $c_1 = 3/2$  and  $c_2 = 11/8$  (P. Pawłowski, unpublished results).

According to the principle of correspondence, the

equations describing an ideal elastic body can be adapted to a viscoelastic body as follows:

$$\hat{j} = \frac{1}{1/\hat{J}_s + 3\tau_0/2d + 11R/8d\hat{J}_i}, \quad (11)$$

where  $\hat{J}$ ,  $\hat{J}_s$ ,  $\hat{J}_i$  are results of Laplace transformations of the functions describing the effective response of the membrane, the response of the membrane itself and the response of the cellular interior, respectively.

Temporal evolution of membrane deformation was obtained using reciprocal Laplace transformation. Then:

$$\frac{z - R}{R}(t) = \mathcal{L}^{-1}[\hat{J}\hat{\sigma}_s^{\text{extr}}], \quad (12)$$

where  $\hat{\sigma}_s^{\text{extr}}$  is the Laplace transformation of the extremal stress,  $\sigma_s^{\text{extr}}$ .

In terms of a model, Eq. 11 describes two viscoelastic units in parallel with an elastic one. It takes into account different factors involved in the general response of the cell to the applied stress. It may be used in a simplified form, depending on our knowledge about the role of the above factors in the investigated process.

## RESULTS

### Experimental procedures

The experimental set-up and *N. crassa* (slime) cells have previously been described (Fikus et al., 1985, Fikus and Pawłowski, 1989). Before the experiment, cells were of roughly spherical shape with a smooth surface as examined under a light microscope and in an electron microscope (Scarborough, 1978). Cells were suspended in 10% sorbitol (Merck, Darmstadt) between two parallel platinum wire electrodes and driven to one of the electrodes by electric field of 1  $V_{pp}$  and 3 MHz. Field strength was adequate for dielectrophoretic alignment of cells; the value of their initial deformation averaged for whole population was smaller than its standard deviation and it did not evolve with time. Field frequency corresponded to the flat maximum of the function describing the relationship between shear stress and electric field frequency (Fig. 1).

Field amplitude was increased stepwise to the desired value, maintained for 60 s and abruptly reduced to the initial, 1  $V_{pp}$  value. Field strength in the experimental chamber was monitored throughout the experiment. The shape of cells was recorded on videotape (final magnification 1,340  $\times$ ). Time points for measurements were chosen so as to best reproduce the evolution of deformation.

Cells were measured in the plane of electrodes in  $z$

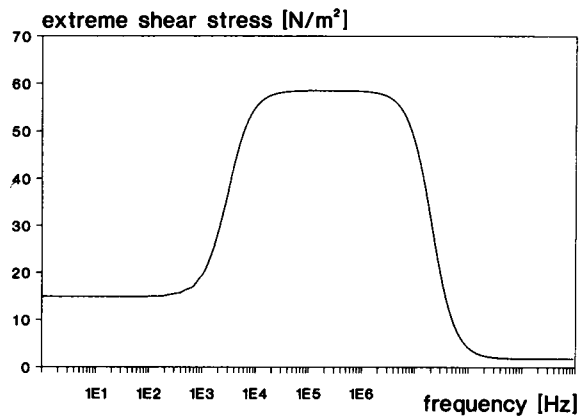


FIGURE 1 Calculated relationship between extreme shear stress in *N. crassa* membrane and electric field frequency (Pawłowski and Fikus, 1991). Cell radius,  $R = 15 \mu\text{m}$ , field strength  $10^4 \text{ V/m}$ .

direction parallel to the field lines. 30 randomly chosen cells were examined within the electric field strength range or  $3\text{--}11 V_{pp}$ . For each cell the field amplitude was calculated at a point distant from the electrode by the initial cell radius (Fikus and Pawłowski, 1989). Temporal trajectories of deformation for all cells were examined and those cells whose deformation did not exceed the measurement noise were disregarded in further analysis. Preliminary experiments suggested that the discarded cells were those which took up substances not penetrating into living membranes.

Original statistical computer programs based on Brandt's (1970) textbook were developed.

### Statistical treatment of the experimental data. Calculation of creep

Systematic experimental errors in measurements of single cells arise from errors in determination of values for: cell radius, field strength, distance between electrodes, relevant physical constants of the system studied, and time of experiment. These partial errors are reflected in the calculated stress as well as in the measured deformations, both of which are used in calculations of rheological parameters. It is not possible to evaluate errors in the calculated value of stress on account of the complex nature of the dependence of stress on measured parameters. Moreover, the correctness of our theoretical approach has to be assumed. These errors, however, are considerably smaller than the dispersion of the experimental data (cf Fig. 2A). This suggests that the scattering of the data is mainly due to the biological diversity of cells studied.

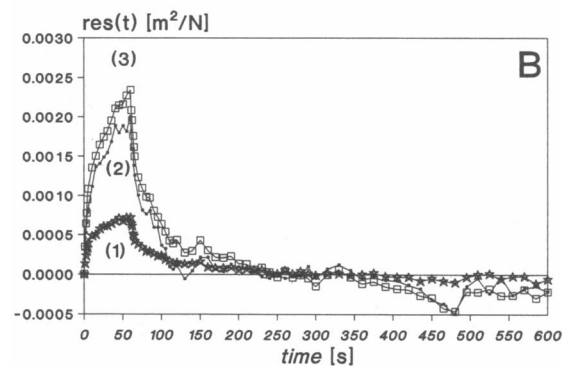
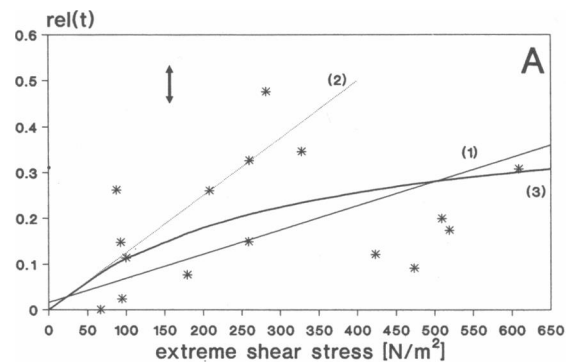


FIGURE 2 Illustration of fitting procedures for determining the response function. (A) Fitting procedures in the 15th s of the experiment. Experimental values of the relationship of  $\text{rel}(t)$  to  $\sigma_i^{\text{ext}}$  for all cells at a given time point were analyzed by various fitting procedures: (1) linear regression for all data (see text, procedure a) (2) linear regression, for data obtained under small stress (see text, procedure b) (3) nonlinear regression according to Eq. 14.  $\text{rel}(t)$  values greatly vary for different cells under similar stress. The bidirectional arrow represents the mean error of experimental measurements of deformations. (B) Response functions obtained from the experimental data analyzed according to Fig. 2A for all time points, following the three proposed regression procedures. The respective values of  $\text{res}(t)$  are denoted by geometrical symbols.

It can be seen that systematic errors will only result in scaling up/down the stress values, leading to proportional changes in the values of amplitudes of deformation (see below), without changing their ratio and their characteristic times.

At the starting point for the statistical analysis, we accept the notion that infinitesimal stress and deformation are linearly dependent (Eq. 7). From the theoretical standpoint, infinitesimal stress should be applied to cells, to obtain their infinitesimal deformation empirically. However, this approach calls for the arbitrary decision about the "infinitesimal" range of both phenom-

ena. In this study a statistical procedure, based on regression analysis, is proposed, solving this problem. It aims at obtaining information about the linear range of stress-deformation dependence from the measurements of finite (measurable) deformations. Stress increments,  $\Delta\sigma_{si}^{extr}$  ( $i = 1, \dots, N$ ), for individual cells were calculated as a function of two parameters: cell radius and the increment of square electric field strength, making use of some constants (cf Appendix). For each cell ( $i = 1 \dots N$ ), at all time points ( $j = 1 \dots M$ ) the relative elongation,  $rel_i^j$ , based on measurements of temporal evolution of cell  $z$  demi-axis, was calculated:

$$rel_i^j = \frac{z_i^j - z_i^c}{R_i}, \quad (13)$$

where  $R_i = [(x_i^c)^2 z_i^c]^{1/3}$  and  $x_i^c, z_i^c$  are demi-axes of a cell before deformation in perpendicular and parallel orientation, respectively, to the field direction,  $z_i^c$  is the demi-axis of the cell, parallel to the field direction at a given time point.

For each moment,  $j$ , the dependence of  $rel_i^j$  on  $\Delta\sigma_{si}^{extr}$  for all cells was found. Three different statistical procedures for data evaluation were considered consecutively:

(a) Linear regression to the set of all  $rel_i^j$  and  $\Delta\sigma_{si}^{extr}$  values was applied and the results verified by Fischer's test. The level of significance was 0.03–0.07 for the first 120 s of the experiment and 0.2–0.3 for the total experimental time. This result did not permit rejection of the assumption about the linearity of the stress to deformation relationship but it did emphasise the considerable scattering of the data exceeding estimated experimental errors (Fig. 2A, curve 1) and suggested the need for development of a different analytical procedure.

(b) Linear regression, as above, was limited to the set of data obtained in the range of small stresses,  $\Delta\sigma_{si}^{extr} \leq 200 \text{ N/m}^2$ . However this procedure fails to include most of the results and as such was found inappropriate (Fig. 2A, curve 2) leading to the development of a nonlinear function.

(c) The nonlinear function used was of the form:

$$rel(t) = \frac{res(t)\Delta\sigma_{si}^{extr}}{1 + \Delta\sigma_{si}^{extr}/\sigma_c}, \quad (14)$$

where  $\sigma_c$  is the characteristic stress fitted to give the best agreement between estimated  $res(t)$  and the results of procedure (b). (Fig. 2B, curves 2 and 3), which for this set of data was found equal to  $500 \text{ N/m}^2$ . Eq. 14 describes all the experimental data. According to Fisher's test, the significance level was 0.01–0.04 for the first 120 s of the experiment and 0.2–0.3 for the whole experimental period; this result did not permit rejection of Eq. 14.

The use of this nonlinear procedure enabled extrapolation of all the experimental data to the range of infinitesimal stress, allowing for the use of the analysis of small deformations for data evaluation. Formally, extrapolation procedure limits our attention to the first term of resolution of Eq. 14 which is consistent with Eq. 7.

$$rel(t) = \frac{res(t)\Delta\sigma_{si}^{extr}}{1 + \Delta\sigma_{si}^{extr}/\sigma_c} \approx res(t)\Delta\sigma_{si}^{extr} + \dots \quad (15)$$

Introduction of nonlinear analysis in the evaluation of the relationship between  $rel(t)$  and  $\Delta\sigma_{si}^{extr}$  resulted in a substantial reduction of residual errors and of the standard deviation of  $res(t)$ . The above procedure, applied to a given set of results (Fig. 2B), permitted assignment of the averaged value of  $res(t)$ , together with its variance, to the whole population of cells studied. Consequently, a region defined by standard deviations was determined within which creep function trajectories for most of the single cells should be found. All data obtained under stress up to  $600 \text{ N/m}^2$  applied for  $t \leq 60 \text{ s}$  could be included in analysis. Fig. 2 shows that the linear regression (procedure [b]) can be used for the analysis of results in the range of stress  $\Delta\sigma_{si}^{extr} \leq 100 \text{ N/m}^2$  (Fig. 2A) acting on cells with  $t \leq 60 \text{ s}$  (Fig. 2B).

## DISCUSSION

In their studies of the mechanical properties of human erythrocytes exposed to an alternating electric field, Sackmann and co-workers (Engelhardt and Sackmann, 1988, Sackmann et al., 1984) have calculated the mechanical stress for undeformed spherical cells, but have measured finite deformations. Furthermore, these authors have evaluated rheological parameters using an approximate, nonlinear constitutive equation which describes the viscoelastic effects. Within the range of infinitesimal deformations, this equation is not reducible to a linear one. This may result in substantial errors in the values of the parameters studied. Moreover, the agreement between these values and those obtained by other methods may be incidental.

In the present work, a statistical procedure was developed which permitted extrapolation of data down to the limit of infinitesimal deformations. Thanks to this procedure, calculations of stress generated in the spherical cell were formally warranted. Furthermore, it ensured that only linear phenomena were included in the analysis which uses linear equations for describing viscoelastic effects.

This procedure allows for high reliability for the final data and substantially reduces statistical errors. Conse-

quently an appropriate rheological model could be fitted to the experimental data. This may be exemplified by our own results.

We have previously analyzed large deformations of *N. crassa* cells, and we described them by the Burgers model (Fikus and Pawłowski, 1989). The model includes a free viscous element, and the fast component of deformation is approximated by a spring element. Owing to the present procedure, the errors were reduced. Consequently, the presence of a pure elastic response and viscous dissipation can no longer be statistically confirmed. Instead, the whole process of deformation could be modeled exclusively by viscoelastic elements.

In the search for an appropriate general rheological model, a typical statistical procedure was applied to fit the theoretical curve (Eq. 8) to the experimental data extrapolated to the infinitesimal stress range according to the nonlinear regression procedure, and to minimize  $\chi^2$ . The whole covariance matrix for the final results was calculated, together with the errors of the values of the parameters estimated. The response function (Eq. 8) was formulated in the monoexponential form:

$$J(\zeta) = A[1 - \exp(-\zeta/\tau)], \quad (16)$$

where  $A$  is the amplitude of the response function,  $\zeta$  is variable and expressed in time units, and  $\tau$  is characteristic time. This function corresponds, in terms of rheological models, to the Voigt-Kelvin model; the values of  $\chi^2 = 140$ ,  $n = 54$ ; large deviations of the experimental data from the theoretical curve were observed (data not shown). These results were unsatisfactory, indicating the need for a more extended rheological model to fit our experimental data.

The function of the form:

$$J(\zeta) = A_1[1 - \exp(-\zeta/\tau_1)] + A_2, \quad (17)$$

was examined. There are two different reduced rheological models which correspond to the function (Eq. 17):

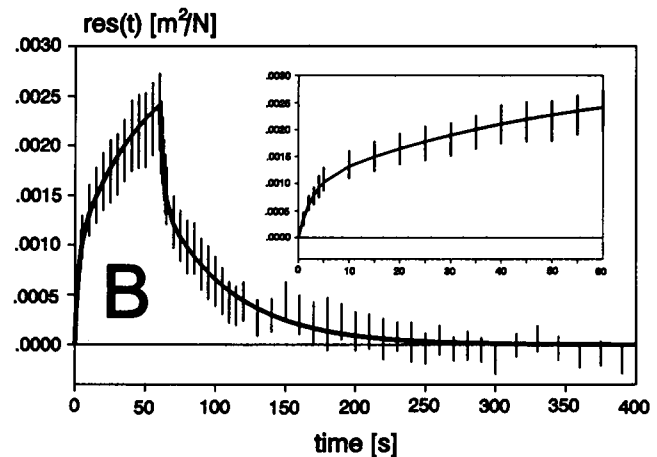
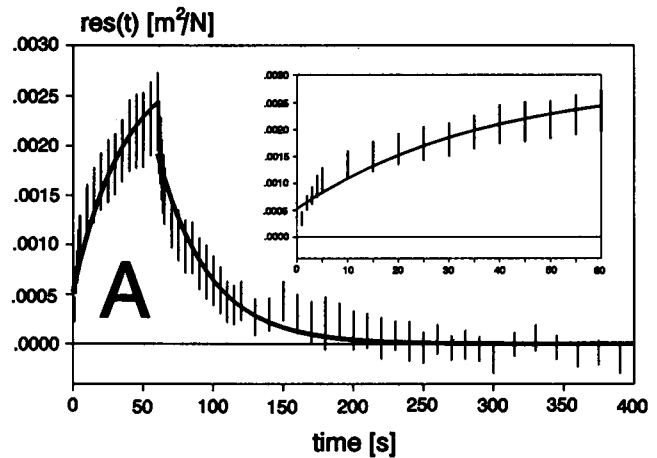
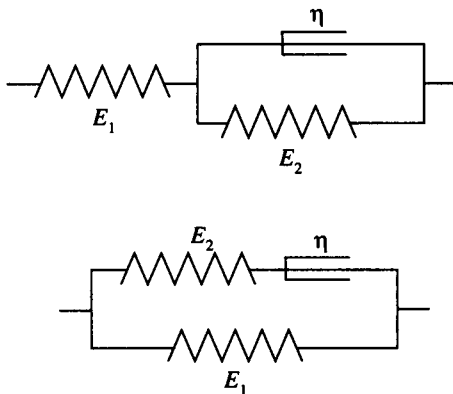


FIGURE 3 Fitting of the function (Eq. 17) (A) and of the biexponential function (Eq. 18) (B) to the experimental data for the whole experimental period and for the first 60 s (inserts) of the experiment. Vertical bars are standard deviations of determined creep values. They determine the width of the area, equal  $[s^2]^{1/2}(t)$  where all the expected trajectories of creep for most cells in the population will be found. The function corresponding to the proposed biexponential rheological model passes through this area (solid line), as proved by the  $\chi^2$  test.

The value of  $\chi^2$  decreased, whereas systematic deviations of the experimental results from the theoretical function, occurring mostly at the first stages of the experiment, were still present (Fig. 3A).

Expanding function (Eq. 17) to the biexponential form:

$$J(\zeta) = A_1[1 - \exp(-\zeta/\tau_1)] + A_2[1 - \exp(-\zeta/\tau_2)], \quad (18)$$

leads to a satisfactory approximation of the theoretical curve to the data ( $\chi^2 = 16$ ,  $n = 52$ ) (Fig. 3B). This function can be represented by four rheological models:

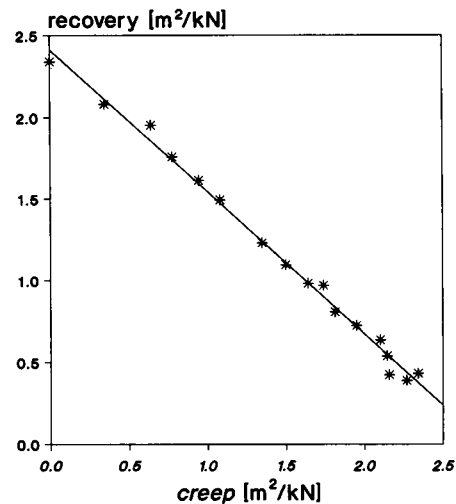
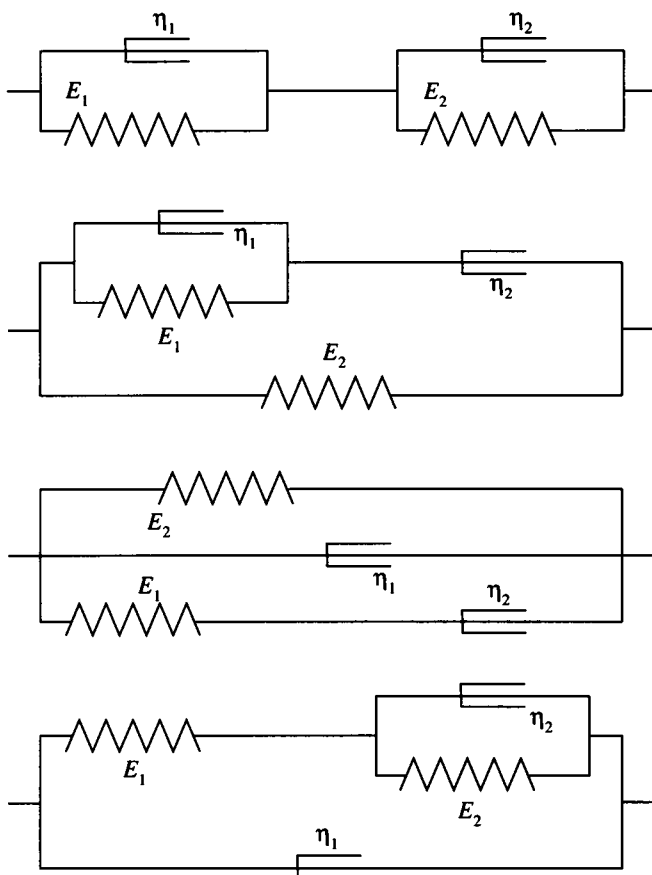


FIGURE 4 Res( $t$ ) values for creep and recovery taken from Fig. 2 *B*, curve (3), corresponding to the same time points for both these processes.

The linear relationship between  $\text{res}(t)$  for creep ( $t_1 < t < t^\dagger$ ) and  $\text{res}(t)$  for stress relaxation ( $t^\dagger < t$ ) (Fig. 4) strongly suggested that both processes could be described by identical temporal functions. In other words, no pure viscous flow was observed, and the time constants for both processes were identical. This result strongly suggests that under the applied stress only reversible, nondamaging viscoelastic deformations were developed and analyzed. As we have shown recently in our laboratory, increase of the stress value and/or prolongation of its duration results in changes in the integrity of the cellular membrane with simultaneous loss of the above temporal symmetry.

We believe that at the present state of our investigations there are no sound foundations for giving preference to any one of the rheological models presented above and, moreover, for relating its elements with any particular cellular structure. This does not rule out further interpretation of our data. According to the biexponential function, two phases of the cellular response, the fast and slow one, can be distinguished in one experiment. They are characterized by two retardation times,  $\tau_1 = 3.0 \pm 0.5$  s and  $\tau_2 = 39 \pm 8$  s,

respectively, and by two amplitudes,  $A_1$  and  $A_2$ , included in Eq. 18. Both the retardation times and the ratio of the amplitudes are independent of the stress calculation method (see Fig. 2 *B*). The fourth parameter of the function (Eq. 18), i.e., the sum of the amplitudes of both responses, depends on the stress calculation method.

The above interpretation of the results enables a comparison of the material-related properties of different cells, independently of the chosen mechanical model of the cell. When the model of a homogeneous sphere with its viscoelastic properties, averaged for its total volume (Skalak et al., 1984, Sung et al., 1988), has been applied to investigations of human leukocytes displaying local small deformations under relatively large stress, two retardation times have been determined for both the fast and slow phase of deformation ( $\tau_1 \approx 2$  s,  $\tau_2 \approx 45$  s, respectively). These phases have been defined in separate experiments; in an analysis of the initial phase of deformation, the authors neglected the systematic deviations of the data from the theoretical curve, (Sung et al., 1988) resembling qualitatively those found in the present work (Fig. 3 *A*).

It remains an open question which cellular structures reponse to stress. In their recently formulated cortical shell-liquid core model, Yeung and Evans (1989) related cell deformation to the viscous interior of the cell and its surface tension. This model has been applied in investigations of human granulocytes (Evans and Yeung, 1989). However, the experimental conditions of stress application in Evans and Young's study, as well as the

magnitude and range of cell deformation differ substantially, from those applied by Skalak et al. (1984), Sung et al. (1988), and in this work. As a result, distinct cellular elements have responded in the various experiments to the stress and consequently, the evaluated parameters corresponded to different phenomena. Moreover, large deformation of the whole cell in the micropipette as analyzed by Evans and Yeung (1989) may result in destruction of the contractile elements in the cellular interior. For this reason, surface tension should be considered to be an important stabilizing factor of cell shape (Evans and Yeung, 1989).

In a separate experiment we observed that *N. crassa* cells subjected to the stress for 180 s do not return to their initial spherical shape after removal of stress. This suggests that the contractile role of surface tension in *N. crassa* cells could have been overlooked. Under conditions of small deformations, the local displacement of cytoplasm is negligible as is the influence of cytoplasm viscosity on the process.

Therefore, we assume that in our experiments the main contribution to the effective viscoelastic response of the cell originates from the cytoplasmic membrane coupled to the membrane skeleton, i.e.,  $\hat{J} = \hat{J}_s$  (Eq. 11).

The proposed rheological model for an averaged population of cells subjected to nondamaging stress can be considered as a starting point for further studies on the origins of the rheological diversity of single cells.

## APPENDIX

### Values and constants used in calculations

|   |  |
|---|--|
| $d_m = 10^{-8} \text{ m}$   | cell membrane thickness                    |
| $\text{Re} \begin{Bmatrix} i \\ e \end{Bmatrix} = 45 \epsilon_0$  | dielectric permeability                    |
| $\text{Re} \begin{Bmatrix} s \\ e \end{Bmatrix} = 7.9 \epsilon_0^*$   |  |
| $\text{Re} \begin{Bmatrix} e \\ e \end{Bmatrix} = 80 \epsilon_0^*$  |  |
| $\text{Re} \begin{Bmatrix} i \\ s \end{Bmatrix} = 0.229 \text{ S/m}$  | specific electric conductivity             |
| $\text{Re} \begin{Bmatrix} e \\ s \end{Bmatrix} = 0.001 \text{ S/m}$  |  |
| $\text{Re} \begin{Bmatrix} s \\ s \end{Bmatrix} = \text{Im} \begin{Bmatrix} i & s & e & i & s & e \\ e & s & e & s & e & s \end{Bmatrix} = 0$ |  |
| $\epsilon_0 = 8.8542 \cdot 10^{-12} \text{ F/m}$  | vacuum dielectric permeability             |
| $\omega/2\pi = 3 \cdot 10^6 \text{ Hz}$   | electric field frequency                   |
| $U = 3,4,5,7,9,11 \text{ V}_{pp}$   | electric field strength between electrodes |
| $R_e = 241.8 \cdot 10^{-6} \text{ m}$   | electrode radius                           |
| $d = (210.1 \mp 27.5) \cdot 10^{-6} \text{ m}$  | distance between electrodes                |

Indices  $i, s, e$  are for cytoplasm, membrane and external medium, respectively. \*Experimentally determined values for a cell suspension (Fikus et al., 1987).

This work was supported within the Research and Development Project (CPBR 3.13) of the Polish Academy of Sciences.

Received for publication 21 May 1990 and in final form 18 October 1991.

## REFERENCES

- Aaronson, L. R., and C. E. Martin. 1983. Temperature-induced modifications of glycosphingolipids in plasma membranes of *Neurospora crassa*. *Biochim. Biophys. Acta.* 735:252–258.
- Barnaby, E., G. Bryant, E. P. George, and J. Wolfe. 1988. Deformation and motion of cells in electric fields. Theory and experiments. *Stud. Biophys.* 127:45–52.
- Brandt, S. 1970. Statistical and Computational Methods in Data Analysis. North-Holland Publishing Company, Amsterdam. Polish Edition, PWN, 1976. 259 pp.
- Emerson, S. 1963. Slime. A plasmodioid variant of *Neurospora crassa*. *Genetica.* 34:162–182.
- Engelhardt, H., and E. Sackmann. 1988. On the measurement of shear elastic moduli and viscosities of erythrocyte plasma membranes by transient deformation in high frequency electric fields. *Biophys. J.* 54:495–508.
- Evans, E. A., and R. Skalak. 1980. Mechanics and Thermodynamics of Biomembranes. CRC Press, Boca Raton, Florida. 254 pp.
- Evans, E., and A. Yeung. 1989. Apparent viscosity and cortical tension of blood granulocytes determined by micropipet aspiration. *Biophys. J.* 56:151–160.
- Fikus, M., E. Grzesiuk, P. Marszałek, S. Różycki, and J. Zieliński. 1985. Electrofusion of *Neurospora crassa* slime cells. *FEMS (Fed. Eur. Microbiol. Soc.) Lett.* 27:123–127.
- Fikus, M., P. Marszałek, S. Różycki, and J. Zieliński. 1987. Dielectrophoresis and electrofusion of *Neurospora crassa* slime. *Stud. Biophys.* 119:73–76.
- Fikus, M. 1988. Cells in a periodic electric field. An analysis of deformation. *Stud. Biophys.* 127:37–44.
- Fikus, M., and P. Pawłowski. 1989. Bioelectrorheological model of the cell. 2. Analysis of creep and its experimental verification. *J. Theor. Biol.* 137:365–373.
- Marszałek, P., J. Zieliński, and M. Fikus. 1989. Experimental verification of a theoretical treatment of the mechanism of dielectrophoresis. *Bioelectrochem. Bioenerg.* 22:289–298.
- Marszałek, P., J. Zieliński, M. Fikus, and T. Y. Tsong. 1991. Determination of electric parameters of cell membranes by a dielectrophoresis method. *Biophys. J.* 59:982–987.
- Nash, G. B., and H. J. Meiselman. 1983. Red cell and ghost viscoelasticity. Effects of hemoglobin concentration and in vivo aging. *Biophys. J.* 43:63–74.
- Pawłowski, P., and M. Fikus. 1989. Bioelectrorheological model of the cell. 1. Analysis of stresses and deformations. *J. Theor. Biol.* 137:321–337.
- Pawłowski, P., and M. Fikus. 1991. Shear deformation of the spherical shell acted on by an external alternating electric field: possible applications to cell deformation experiments. *Z. Naturforsch.* 46c:487–494.
- Sackmann, E., H. Engelhardt, K. Fricke, and H. Gaub. 1984. On dynamic molecular and elastic properties of lipid bilayers and biological membranes. *Colloids Surf.* 10:321–335.
- Scarborough, G. A. 1978. The *Neurospora* plasma membrane: a new experimental system for investigating eukaryote surface membrane



- 
- structure and function. *In Methods in Cell Biology*, Vol. 20. D. M. Prescott, editor. Academic Press, San Diego. 117-133.
- Skalak, R., S. Chien, and G. W. Schmid-Schönbein. 1984. Viscoelastic deformation of white cells. Theory and analysis. *In White Cell Mechanics: Basic Science and Clinical Aspects*. Alan R. Liss, Inc., New York. 3-18.
- Sung, K. L. P., C. Dong, G. W. Schmid-Schönbein, S. Chien, and R. Skalak. 1988. Leukocyte relaxation properties. *Biophys. J.* 54:331-336.
- Waugh, R. E. 1987. Effects of inherited membrane abnormalities on the viscoelastic properties of erythrocyte membrane. *Biophys. J.* 51:363-369.
- Waugh, R. E., and P. Agre. 1988. Reductions of erythrocyte membrane viscoelastic coefficients reflect spectrin deficiencies in hereditary spherocytosis. *J. Clin. Invest.* 81:133-141.
- Yeung, A., and E. Evans. 1989. Cortical shell-liquid core model for passive flow of liquid-like spherical cells into micropipets. *Biophys. J.* 56:139-149.